# The relationship between hemorrhagic fever with renal syndrome cases and time series of NDVI in Dayangshu District

**YAN Lei[1†], HUANG Hua-guo[2†], ZHANG Wen-yi[3†], WANG Jian-bo[4], REN Yu-huan[5], FANG Li-qun[3], HUANG Xiao-xia[1], CAO Wu-chun[3], YAN Shou-yong[5], WANG Shi-wen[1]**

1. *Institute for Viral Disease Control and Prevention, Chinese Center for Disease Control and Prevention, Beijing* 100052, *China*;
2. *State Key Laboratory for Silviculture and Conservation, Jointly Sponsored by Ministry of Education and College of Forestry of Beijing Forestry University, Beijing* 100083, *China*;
3. *Beijing Institute of Microbiology and Epidemiology, State Key Laboratory of Pathogen and Biosecurity, Beijing* 100071, *China*;
4. *Public Health Center, Da Xin An Ling Bureau of Forest, Inter Mongolia Hulunbeier* 022150, *China*;
5. *State Key Laboratory of Remote Sensing Science, Jointly Sponsored by the Institute of Remote Sensing Applications of Chinese Academy of Sciences and Beijing Normal University, Beijing* 100101, *China*

**Abstract:** In China, hemorrhagic fever with renal syndrome (HFRS) is still endemic in 31 of 32 provinces, autonomous regions and metropolis, and accounts for 90% of the HFRS cases reported globally. Some studies indicated that HFRS incidence was significantly different among different precipitation, temperature level, land-cover, soil types and normalized difference vegetation index (NDVI). The current study proposed to explore the temporal relationship between the inter-annual variation in the number of cases of human disease caused by hantavirus and time series of NDVI in order to predicate the trend and level of the case number of HFRS. Dayangshu district in Inner Mongolia Autonomous Region was selected as the study area. Based on Landsat TM image, the land-use of this district was divided into four categories: hill, forest, farm-land and residence area. The relationship between the case number of HFRS and time series NDVI was explored by using graphic demonstration, correlation test and linear regression analyses. The study indicated that the highest correlation coefficient was 0.67 (P value<0.001) between three months backward NDVI and the number of cases of HFRS in farmland. The result also indicated that the peak of cases happened 3 months later than the peak of monthly NDVI. This study quantified the temporal relationship between NDVI and the number of the cases of HFRS.

**Key words:** remote sensing, HFRS, SPOT, NDVI

**CLC number:** R181.8/TP79 **Document code:** A

Hemorrhagic fever with renal syndrome (HFRS) is a zoonosis caused by different species of *Hantavirus* (HV). It was first recognized in northeastern China in 1931 and has been prevalent in many other parts of China since 1955. At present, HFRS is still endemic in 31 of 32 provinces, autonomous regions and metropolis, and accounts for 90% of the HFRS cases reported globally. During the endemic period, the incidence is 3.5/100,000 in the endemic areas and the mortality rate closed to 3% (Song *et al*., 1998; Zhi *et al.*, 1998). The author chooses Dayangshu district as study area to apply the usage of remote sensing and GIS in the area of HFRS prevention.

## 1 BACKGROUND

Remote sensing and GIS were used in the HFRS study since 1990s. Glass *et al*. (2000) conducted a study to prove the hypothesis that the 1993 U.S. hantavirus pulmonary syndrome (HPS) outbreak was attributed to environmental conditions and increased rodent populations caused by unusual weather in 1991—1992. They estimated precipitation at 28 HPS and 170 control sites during the springs of 1992 and 1993 and compared it with precipitation during the previous 6 years by using rainfall patterns at 196 weather stations, they also used elevation data and Landsat Thematic Mapper satellite imagery collected the year before the outbreak to estimate HPS risk by logistic regression analysis. The result shows that rainfall at case sites was not higher during 1992—1993 than in previous years. But the elevation showed association between environmental conditions and HPS risk the following year. Repeated analysis using satellite imagery from 1995 showed substantial decrease in me-

**Received**: 2008-08-02; **Accepted**: 2008-12-03

**Foundation**: China National Funds for Distinguished Young Scientists (No. 30725032); The National Natural Science Foundation of China (No. 30590374, 30700682); China National Funds for Communicable Diseases (No. 2008ZX1004-012).

**First author biography**: YAN Lei (1973— ), a PhD with MD and MPH background. He graduated from State Key Laboratory of Remote Sensing Science, Jointly Sponsored by the Institute of Remote Sensing Applications of Chinese Academy of Sciences and Beijing Normal University. His research interests include application of geospatial information techniques to public health, especially to infectious diseases. Now, He works in Institute for Viral Disease Control and Prevention, Chinese Center for Disease Control and Prevention.

**Corresponding author:** WANG Shi-wen, E-mail: wangshiwencdc@163.com

dium- to high-risk areas. Only one case of HPS was identified in 1996. Boone *et al*. (2006) tested environmental data from remote sensing and geographic information system maps as indicators of Sin Nombre virus (SNV) infections in deer mouse (*Peromyscus maniculatus*) populations in the Walker River Basin. They determined by serologic testing the presence of SNV infections in deer mice from 144 field sites. They also used remote sensing and geographic information systems data to characterize the vegetation type and density, elevation, slope, and hydrologic features of each site. The data retroactively predicted infection status of deer mice with up to 80% accuracy. They believe that if the models of SNV temporal dynamics can be integrated with baseline spatial models, human risk for infection may be assessed with reasonable accuracy. In China, Fang *et al*. (2003a) used landsat-7 TM images to analysis the spatial distribution of HFRS cases in Haidian district. They found the HFRS cases' distribution was not randomly and related with geographic characters. Fang *et al*. (2003a) also used SPOT4 NDVI data as background to match the HFRS disease data, and found that the HFRS incidence correlated with NDVI values ($r=0.417$, $P<0.001$). Fang *et al*. (2004, 2006) used GIS to map the different type of HFRS' distribution in China. Yan (2007a, 2007b) also analyzed the relationship between the HFRS incidence and land cover, soil types, temperature, rainfall, NDVI, land surface temperature, and built a remote sensing-ecology model of HFRS. The current study proposed to explore the temporal relationship between the inter-annual variation in the number of cases of human disease caused by hantavirus and time series of NDVI in order to predict the case number of HFRS.

## 2 STUDY AREA AND DATA SETS

Dayagnshu district is located in the inter Mongolia and next to the south foot of Da Xin An Ling. The area of Dayangshu is $1016km^2$ and the area of towns is $23km^2$. The landform of Dayangshu district mainly includes plain area and low hill and the most land is covered by farmland which is for soybean and forest. The population of the district is about 179,000. Among them about 119,000 live in the towns, 30,000 in the rural area and 30,000 are migrants. It was selected as the study area because it is a persistently high risk area for HFRS and all HFRS cases were just infected by Hantaan virus. From 2001 to 2005, there were 150 cases of HFRS and 3 fatal cases, and the mortality rate was 2% (Tang *et al*., 2000; Nashun *et al*., 2002, 2003; Zhai *et al*., 2003; Sasen *et al*., 2006). Almost all the cases were admitted in one biggest hospital and the patients' information were reported timely as well as the surveillance of rodents population density. Therefore it is a good place for study on the temporal relationship between the number of HFRS cases and NDVI.

The data sources are shown in Table 1. Because the notify system of communicable disease were not established before 2004, the patients' information were collected from the Biggest hospital in the dayangshu district.

**Table 1 Data resources description**

| No. | Name | Scale | Year |
|---|---|---|---|
| 1 | Digital maps of Dayangshu | 1∶250000 | 2000 |
| 2 | Patients records | | 2001—2005 |
| 3 | Spot vegetation | 1km | 2001—2005 |
| 4 | Google earth image of Dayangshu | 30m | 2004 |
| 5 | Landsat images | 30 m | 2000 |

## 3 METHODS AND ANALYSIS

The study was divided into two steps: (1) processing long term time series NDVI data; and (2) analyzing the relationship between HFRS and the time series of NDVI.

### 3.1 Processing long term time series data of NDVI

Fig. 1 indicates the procedure of processing the long term time series of NDVI data.

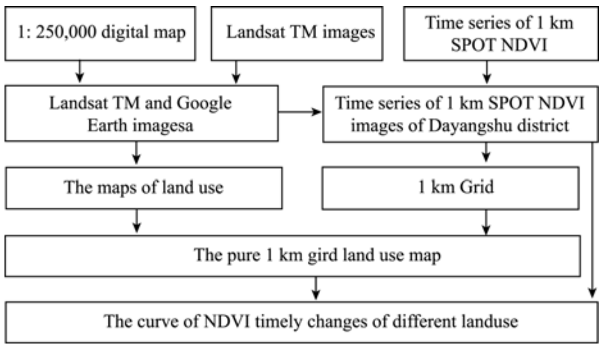


Fig. 1 Flow chart of processing time series of NDVI

(1) To develop digital map (1∶250,000 scale) of Dayangshu district. The map included contour lines, commanding height, paths, rural roads, county roads, provincial roads, national roads, rail ways, rivers (one-way rivers, two-line rivers, streams, lakes, reservoirs, etc.), towns and villages, as well as the border of county. The map was saved to Mapinfo format.

(2) To obtain the Landsat Thematic Mapper (TM) images (2000, 2002) of Dayangshu district from Chinese natural resources database and get Google Earth images of Dayangshu district From Google Earth Pro in 2005. The land-use classification was made by using the two different kinds of images.

(3) To stratify the major type of land-cover of Dayangshu district into four categories: hill grass, forest, farmland and residence area by using Regions of Interest (ROIs) function of Environment for Visualizing Images (ENVI) 4.3 based on Landsat Thematic Mapper (TM) image (2002) and Google earth images.

(4) To produce Normalized Difference Vegetation Index (NDVI) by SPOT vegetation's VGT-S10 (http://free.vgt.vito.be,

10d synthesis). It compiled by merging segments (data strips) acquired in 10d. All the segments of this period are compared again pixel by pixel to pick out the "best" ground reflectance values. These products provide data from all spectral bands, the NDVI and auxiliary data on image acquisition parameters.

(5) To link the Dayangshu landuse map and Spot vegetation image by the pixel's latitude and longitude (Fig. 2). A grid vector map of Dayangshu district was developed based on Spot vegetation image with each pixel 1×1 km$^2$. Each pixel had one value of NDVI. Co-registered and overlaid the vector map on the land-cover map by using latitude and longitude as the fixed points. The average value of NDVI of each type of land-use was calculated. If the grid of land-cover map contained only one land-cover category, the NDVI value of the grid (pixel) was considered the NDVI value of this land-cover category. If the land cover was not the only one category in one grid, the NDVI value of this grid will not be considered. The NDVI value of each land-cover category in Dayangshu district was obtained by adding all NDVI value of each grid of the land-cover category and divided by the number of the grids. The temporal resolution of NDVI was 10d and the value of the date 11$^{th}$ of each month was used in this study as monthly average NDVI value in this study. Since the land use was not changed a lot during the 5 years period, the 2000's land-use map was used to present 2001—2003's status and the 2005's land-use map was used to present 2004—2005's status. If the grid of land-cover map contained only one land-cover category or other types of land covered less than 5%, the NDVI value of the grid (pixel) was considered the NDVI value of this land-cover category. If the land cover was not the only one category in one grid, the NDVI value of this grid will not be considered. The NDVI value of each land-cover category in Dayangshu district was obtained by adding all NDVI value of each grid of the land-cover category and divided by the number of the grids.

### 3.2 Analyzing the relationship between HFRS and the time series of NDVI

There were three steps to reveal the relationship between HFRS and the time series of NDVI. The first step was to visualize comparison through overlapping the curves of the time series of NDVI, the rodent population density and the number of cases of HFRS. The second step was to conduct correlation analysis between the monthly number of HFRS cases and the trends of NDVI with monthly stepwise backward movements. Finally, a model was established to indicate the quantitative relationship between the number of HFRS cases and the optimal time (month) of NDVI.

(1) To make visual comparison by using time series NDVI curves of four types of land cover and the trend of rodent's population density and the bar graphs of the monthly number of the new cases. Using five years' (2001—2005) monthly average value of NDVI, four curves of monthly variation of NDVI of different land-use categories were developed and the bar graph of the cases number of HFRS by months and years was overlaid on the monthly variation in NDVI curves Fig. 3. The abscissa represents month/year, which was from January 2001 to December 2005 and the left ordinate represents the value of monthly NDVI and the right ordinate represents the number of new cases. Fig. 3(a) indicated that the peak of the cases appeared in November no matter how many cases in each year,

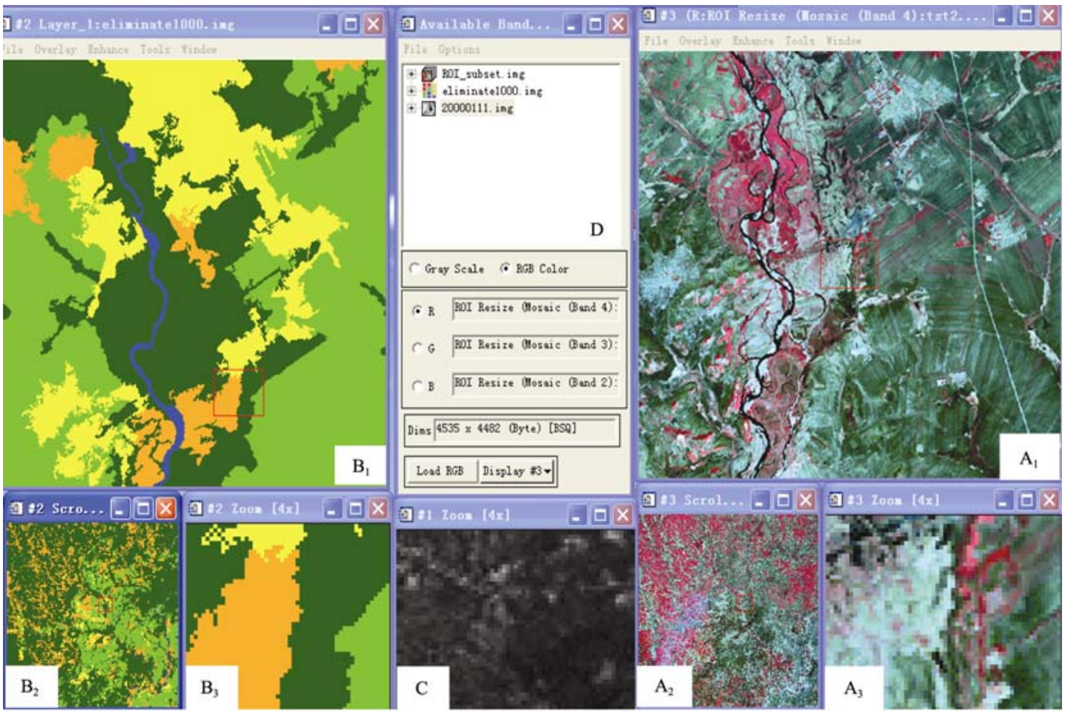


Fig. 2 Dayangshu district's Lantsat TM image, Land use map and NDVI graph

$A_1$, $A_2$, $A_3$: Landsat TM images of Dayangshu; $B_1$, $B_2$, $B_3$: land-use map of Dayangshu; C: SPOT vegetation images; D: interactive interface of ENVI software

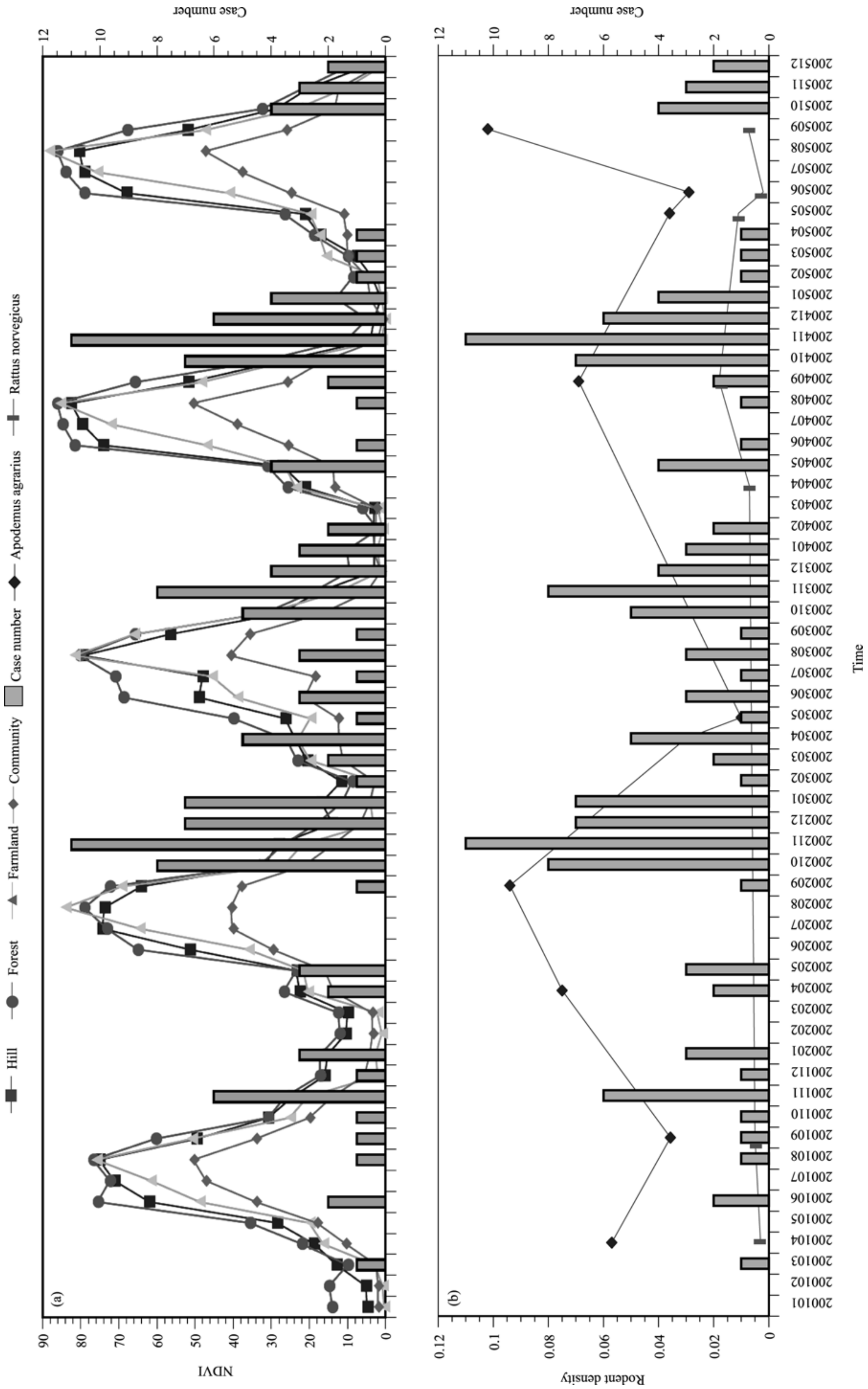


Fig. 3 The relationship between NDVI, rodent density and HFRS cases numbers (2001—2005)

(a) Relationship between NDVI and HFRS cases; (b) Relationship between rodents density and HFRS cases while the peak of NDVI value was in August no matter of the type of land cover. In order to monitor the changes of the rodent population density, the surveillance sites in the district put mousetrap two times (spring and autumn) every year. The successful capture rate of *A.agrarius* in Dayangshu district was also shown in Fig. 3 (b) with the bar graphs of case number of HFRS.

(2) To conduct correlation analysis of the monthly number of new cases with the monthly average value of NDVI. First, graphic analysis was used to find out the relationship between the incidence of HFRS and temporal NDVI. The number of cases in 2004 and the values of temporal NDVI of farm land in 2003 and 2004, as an example, were used to make curves and bar graphs (Fig. 4). The curves of temporal NDVI by 0, 1, 3 and 6 months backward were made to match the bar graphs of the monthly number of new cases of HFRS. Fig. 4 showed that the peak of NDVI of 3 months backward was overlapped with the peak of case number of HFRS.

In order to quantify the relationship between monthly NDVI and the number of cases of HFRS, seven (1—6 months backward) correlation tests were conducted separately. The results of correlation coefficient and P-value were shown in Table 2. The highest correlation coefficient was 0.67, 0.66, 0.66, and 0.61 (P value<0.001) between three or four month backward NDVI and the number of HFRS cases in farmland, hill land, forest and residence area respectively. In the other word, the result indicated that the peak of cases happened three or four months later than the peak of monthly NDVI.

(3) In order to establish model to predicate the risk of HFRS outbreak, the linear regression were conducted between monthly number of cases and three months backward NDVI in farmland. The result was shown in Fig. 5. The linear regression model described the quantitative relationship between the NDVI and the number of cases. It can predict the number of cases by using the monthly NDVI values in the study area.

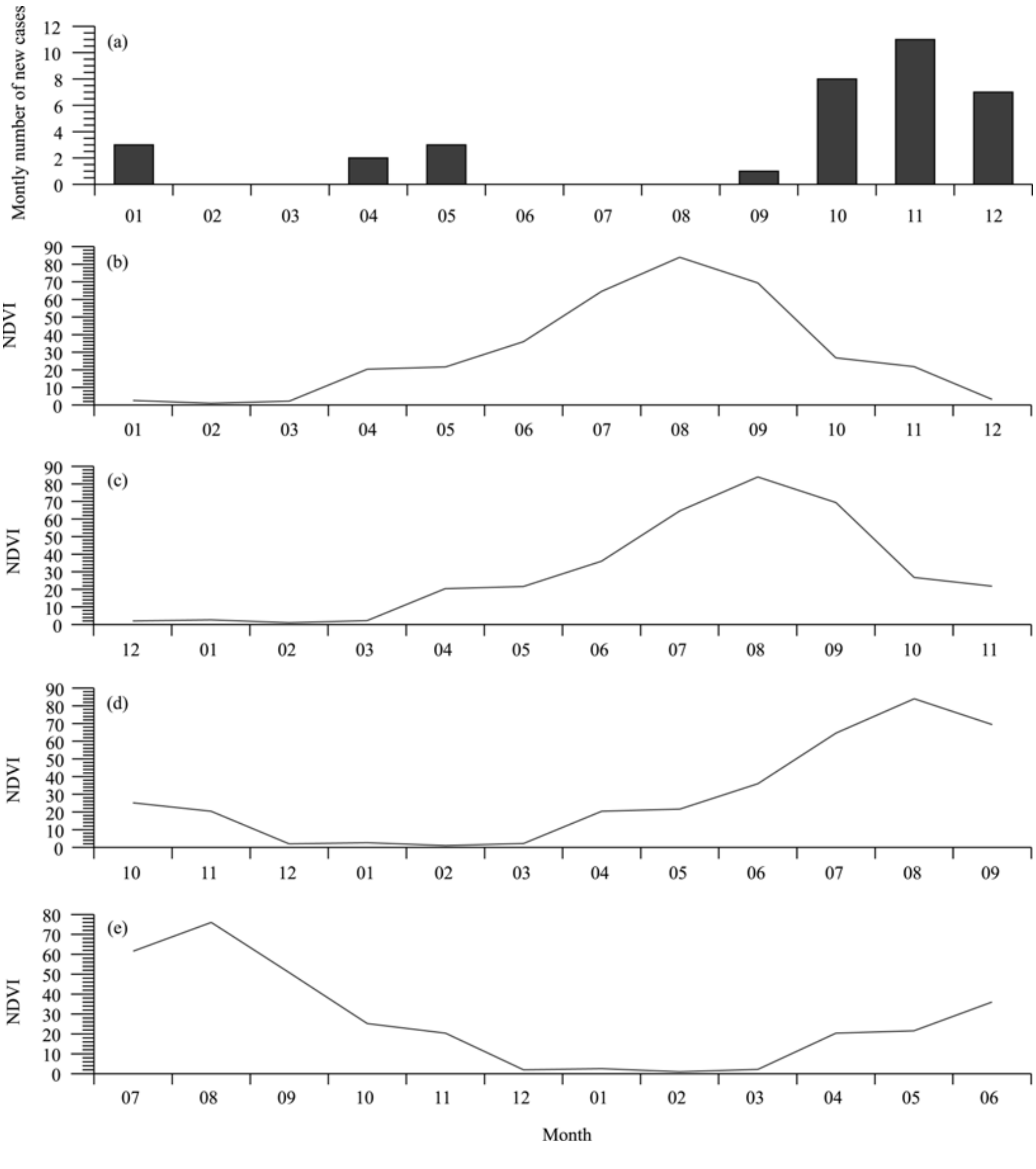


Fig. 4 The relationship between HFRS case numbers and backward NDVI value
(a) HFRS cases; (b) Backward 0 month; (c) Backward 1 months; (d)Backward 3 months; (e) Backward 6 months

**Table 2 Correlation coefficient between monthly NDVI and number of cases of HFRS**

| | 0 month backward | 1 month backward | 2 months backward | 3 months backward | 4 months backward | 5 months backward | 6 month backward |
|---|---|---|---|---|---|---|---|
| Hill land | −0.31 | −0.07 | 0.34 | 0.63 | 0.66 | 0.46 | 0.11 |
| *P*-value | 0.01 | 0.60 | 0.01 | 0 | 0 | 0 | 0.41 |
| Forest | −0.34 | −0.06 | 0.33 | 0.57 | 0.66 | 0.47 | 0.10 |
| *P* -value | 0.01 | 0.64 | 0.01 | 0 | 0 | 0 | 0.44 |
| Farm land | −0.31 | −0.02 | 0.43 | 0.67 | 0.59 | 0.37 | 0.06 |
| *P* -value | 0.02 | 0.90 | 0 | 0 | 0 | 0 | 0.64 |
| Residence | −0.32 | −0.02 | 0.38 | 0.61 | 0.55 | 0.32 | 0.04 |
| *P* -value | 0.01 | 0.86 | 0 | 0 | 0 | 0.01 | 0.74 |

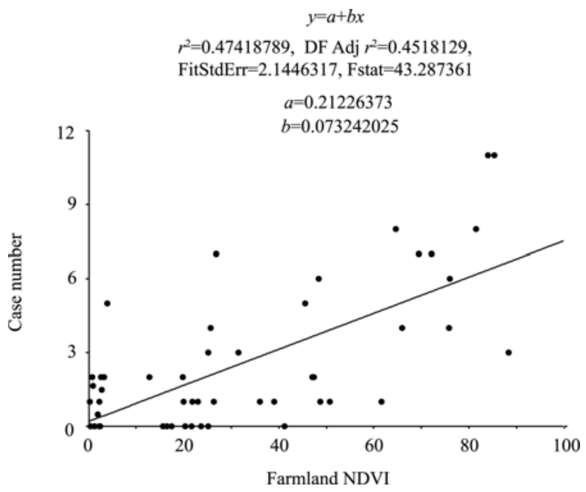


Fig. 5 Scatter graph of 3 month backward farm land NDVI values and case number of HFRS

## 4 DISCUSSION

Several studies have investigated that the onset, intensity and duration of vegetation greenness were part of the major conditions to influence the incidence or number of cases of vector bond diseases. NDVI is a good indicator of the vegetation. It was also recognized that a marked seasonal change in NDVI values and the number of HFRS cases related to Hantavirus. There was few studies to quantify the temporal relationship between NDVI and the number of the cases of HFRS.

In this study, Fig. 3 showed that the peak of monthly NDVI was 3—4 months earlier than the peak of monthly number of cases in four land-use categories in Dayangshu clearly. Six months backward correlation test gave the same evidence and also quantified the results again.

The life circle of *A.agrarius*, the host of Hantaan virus, could explain the reason partially. The reproductive circle of *A.agrarius* is 4 times per year and the infantile rats have reproductive potential just three months after birth. They are more productive in spring and fall. The high value of NDVI in the land-use of farm and forest indicated the intensive condition of vegetation greenness. In this condition, the population density of rodent would be increased. After three or four months the hosts of mature rodents increase. The inference was also supported by the age, sex and occupation of the cases. In this study, most cases were male and worked in the field and aged 20—50 years old, because they had more chances to contact the hosts.

Comparing the value of correlation and coefficient between the number of cases and three months backward NDVI among the four categories of land-use in Dayangshu district, the value of farmland was the highest and 50% cases were farmer, the linear regression in the farmland was performed and a model was established. The model can predicate the number of cases in three months advance by using NDVI values in Dayangshu district but the accuracy needs to be test and the model also needs to be improved.

The study quantified the temporal relationship between NDVI and the number of the cases of HFRS. It makes it possible to develop an early warning system for the outbreak of HFRS based on remote sensing data. Meanwhile, it will be useful for providing interventions in advance. For example, the government of Dayangshu provided free vaccine for high risk population in May and June 2005, the number of cases declined significantly.

The limitation of the study was the incomplete data of rodent population, because the mousetrap was installed only two times a year. The successful capture rate could not reflect the change of the rodent population density completely. It is difficult to establish a model to describe the relationship among the person, host and environment.

## REFERENCES

Boone J D, McGwire K C, Otteson E W, DeBaca R S, Kuhn E A, Villard P, Brussard P F and St Jeor S C. 2000. Remote sensing and geographic information systems: charting Sin Nombre virus infections in deer mice. *Emerging Infectious Diseases.*, **6**(3): 248—258

Fang L Q, Cao W C, Chen H X, Wang B G, Wu X M Yang H and Zhang X T. 2003.Study on the application of geographic information system in spatial distribution of hemorrhagic fever with renal syndrome in China. *Chinese Journal of Epidemiology*, **24**(4): 265—270

Fang L Q, Cao W C, Dong Z, Wu X M, Sun P Y, Martin Kulldorff, Wang B C, Yang H and Li X W. 2003. Spatial analysis on the distribution of hemorrhagic fever with renal syndrome by geographic information system in Haidian district, Beijing. *Zhonghua Liu Xing Bing Xue Za Zhi*, **24**(11): 1020—1023

Fang L Q, Li C Y, Yang H, Wu X M, Yang H, Chen H X, Li X W and Cao W C. 2003. Using geographic information system to study on the association between epidemic areas and main animal hosts of hemorrhagic fever with renal syndrome in China. *Chinese Journal of Epidemiology*, **25** (11): 929—933

Glass G E, Cheek J E, Patz J A, Shields T M, Doyle T J, Thoroughman D A, Hunt D K, Enscore R E, Gage K L, Irland C, Peters C J and Bryan R. 2000. Using remotely sensed data to identify areas at risk for hantavirus pulmonary syndrome. *Emerging Infectious Diseases*, **6**(3): 238—247

Nashun Menghe and Chen Y G. 2002. On Forest Classification Management in Dayangshu District *Inner Mongolia Forestry Investation and Design*, **25**(1): 47—48

Nashun Menghe and Li X L. 2000. Protection policy of forest resources in Dayangshu bureau of forest. *Inner Mongolia Forestry Investation and Design*, **24** (3): 21—23

Sasen Gaowa Li C P, Wu S B and Wang J B. 2006. Population structural changesin hemorrhagic fever with renal syndrome patients at Inner Mongolia Xing'an forest area. *Chinese Journal of Pest Control*, **22**(4): 264—265

Song G. 1998. Manual of Hemorrhagic Fever with Renal Syndrome Control and Prevention. Beijing People's Medical Publishing House

Tang L Y, Chen H X, Zou X Y, Luo C W, Yu T, Dong J J, Kang F C and Zhao L Y. 2000. A Surveillances tudy on the enzoonostic natural of HFRS (Hemorrhagic Fever with Renal Syndrome) in Dayangshu district of Elunchun autonomic county. *Chinese Journal of Zoonoses*, **16**(6): 89—90

Yan L. 2007. Ecological Study on Hemorrhagic Fever with Renal Syndrome in China based on Spatial Information technology. Chinese Science of Academy

Yan, L, Fang L Q , Huang H G, Zhang L Q, Feng D, Zhao W J, Zhang W Y, Li X W and Cao W C. 2007. Relationship between landscape elements and Hantaan virus-related hemorrhagic fever with rental syndrome in China. *Emerging Infectious Diseases*， **13**(9): 1301—1306

Zhai X A and Wang L K. 2003. Suggestion on returning cropland back to forestry in Dayangshu Forestry Bureau, Inner Mongolia. *Inner Mongolia Forestry Investation and Design*, **26**(2): 49—50

Zhi H. 1998, Epidemiology. Beijing People's Medical Publishing House

# 肾综合征出血热疫情与 NDVI 的时间关系
## ——以内蒙古自治区大杨树镇为例

闫 磊[1]，黄华国[2]，张文义[3]，王剑波[4]，任玉环[5]，
方立群[3]，黄晓霞[1]，曹务春[3]，闫守邕[5]，王世文[1]

1. 中国疾病预防控制中心 病毒病预防控制所，北京 100052;
2. 北京林业大学 省部共建森林培育与保护重点实验室，北京 100083;
3. 军事医学科学院 微生物流行病研究所，北京 100071;
4. 内蒙古自治区大兴安岭林业中心卫生防疫站，内蒙古 呼伦贝尔 022150;
5. 遥感科学国家重点实验室，中国科学院遥感应用研究所 北京师范大学，北京 100101

摘 要： 利用月度肾综合征出血热发病人数和长时序月度 NDVI 值的相互关系，对肾综合征出血热的发病趋势及发病人数进行预测。研究区大杨树镇 2001—2005 年共有 144 例完整的 HFRS 病人资料，以及同期详细的宿主动物捕获数据。基于 Landsat TM 影像以及 Google earth 影像，大杨树地区土地利用分为 4 种类型，山地、林地、农田以及居民点。各类土地利用类型的 NDVI 数据由 SPOT-4 卫星的 VGT-S10 数据集(10d 最大化合成的 NDVI 数据)提供。对 HFRS 病例与 NDVI 之间的关系进行图解分析、相关分析和回归分析。研究表明，NDVI 的峰值多出现于 8 月，而 HFRS 发病人数的峰值多出现在 11 月。前朔 3 个月的农田 NDVI 值与 HFRS 病例数之间的相关系数为 0.67($P$ 值$<0.001$)。农田 NDVI 峰值比 HFRS 病例的峰值提前了 3 个月。研究量化了 NDVI 与 HFRS 之间的关系，为 HFRS 早期预警系统的建立提供了依据。

关键词： 遥感，肾综合征出血热, SPOT, NDVI

中图分类号： R181.8/TP79 文献标识码： A

## 1 引 言

肾综合征出血热(HFRS)是一种全球性的、由携带不同汉坦病毒的动物(主要是黑线姬鼠、褐家鼠等)所传播的自然疫源疾病，广泛分布于亚洲、欧洲、非洲、南北美洲和大洋洲的 78 个国家。其中，中国是 HFRS 的高发国家，31 个省、自治区和直辖市经血清学确证为 HFRS 的疫区，其发病率为 3.5/10 万左右；在 HFRS 流行期间，病死率高达 3%；全国发病人数占全球病例总数的 90%。HFRS 在中国的分布范围广、疫区类型复杂，是全国法定的二类传染病(宋干等, 1998；志浩等, 1998)。

空间信息技术在出血热研究中的应用在国外起步较早。Glass 等(2000)利用遥感数据，对美国 1993 年暴发的汉坦病毒肺综合征(HPS)的危险地区进行了鉴别，认为这次 HPS 的暴发受环境条件的影响，是 1991—1992 年异常气候导致鼠类数量增加的结果。为此，他们估算了 28 个 HPS 发生地和 170 个对照地 1992 年和 1993 年春季的降雨量，利用 196 个气象站建立的径流模式与前 6 年的降雨量进行比较，利用高程数据和 HPS 暴发前 1 年的 Landsat TM 影像，通过逻辑回归分析估算 HPS 暴发的危险程度。结果表明：案例研究地点 1992—1993 年间的径流量

收稿日期：2008-08-02；修订日期：2008-12-03

基金项目：国家杰出青年基金(编号：30725032)，国家自然基金(编号：30590374, 30700682)和传染病重大专项基金(编号：2008ZX10004-012)。

第一作者简介：闫磊(1973— )，男，助理研究员，1998 年首都医科大学医疗专业毕业，1998—2000 年北京大学第一附属医院医师，2003 年菲律宾国立大学获流行病学硕士学位，2007 年于中国科学院遥感应用研究所获博士学位，现任职中国疾病预防控制中心病毒病预防控制所，从事疾病预防控制和地理流行病学方面的研究工作。

通讯作者：王世文，E-mail: wangshiwencdc@163.com

和前几年相比并没有增大。然而，高程和卫星数据却显示出环境条件与来年的 HPS 危险程度有关。比较由 1992 年和 1995 年卫星影像得到的 1993 年、1996 年 HPS 危险程度图，可以发现其中的高危险区范围在 1996 年显著缩小了。Boone 等(2004)在 144 个野外点上，利用遥感和 GIS 专题图导出的植被类型和密度、海拔高度、坡度以及水文特性等环境数据，作为内华达州和加利福尼亚州的 Walker 河流域里鹿鼠 (*Peromyscus maniculatus*)感染辛诺瓦(Sin Nombre，SNV)病毒的指标。与此同时，他们也对这些点上的鹿鼠是否感染 SNV 病毒，进行血清学方法的检验。根据这些数据，他们回顾性地估算了该地区鹿鼠的感染状况，其精确度达到 80%以上。他们还指出：如果 HPS 的时间动态模型能够和基础空间模型集成在一起，对人类受感染的危险程度进行估算，其精度可以达到合理的水平。在中国，方立群等(2003a)利用 Landsat7 的 TM 遥感图像，对北京市海淀区的肾综合征出血热的空间分布进行了研究，认为其空间分布为非随机分布而且与地理环境因素密切相关。方立群等(2003b)以 1998-06-01 SPOT4 的植被影像为背景，通过 NDVI 与人群发病资料的匹配分析，得出 HFRS 发病率与 NDVI 之间呈正相关($r$=0.417，$P$<0. 01)。他们根据各监测点上 NDVI 的差异，绘制了中国 HFRS 危险区域分布图；对全国 HFRS 进行了空间聚类研究。方立群等(2004, 2006)在 GIS 技术支持下，揭示出中国不同类型的肾综合征出血热的分布，具有明显的区域特性。从中国东北向西南移动，以 I 型汉坦病毒为主的混合型疫区与 II 型汉坦病毒为主的混合型疫区具有交替分布的特征。闫磊等(2007a, 2007b)对全国汉坦病毒相关的肾综合征出血热与景观要素(包括地形、土壤、植被、气候)之间的空间关系进行了研究，建立了肾综合征出血热(HFRS)的遥感生态环境模型，使其研究领域由“病人—带毒鼠—鼠群”扩展到“病人—带毒鼠—鼠群—生态环境”，通过对大杨树镇 HFRS 的流行病学、遥感及其背景等数据的分析，揭示了发病人数、鼠群数量和 NDVI 变化曲线之间的关系。

## 2 研究区域与数据

大杨树镇位于内蒙古自治区呼伦贝尔市境内鄂伦春自治旗南部，大兴安岭东南麓，地处东经 124°10′—124°40′，北纬 49°30′—50°10′，东至本旗古里乡，西邻宜里镇，北接乌鲁布铁镇，南与莫力达瓦达斡尔族自治旗毗连。行政辖区面积 1016km$^2$，镇区面积 26km$^2$。镇区依山傍水，雄居于甘河北岸的冲积平原，地势起伏比较和缓，土地利用类型单纯、农作物地块面积大，属城乡结合型的田园城镇。全镇共辖 20 个居委会，34 个行政村，以农牧业为主导产业，镇区人口 11.9 万人，农业人口 3 万人，流动人口 3 万余人，分属蒙、汉、回、鄂伦春、鄂温克、达斡尔、满、朝鲜、锡伯、壮等 13 个民族。这里是以黑线姬鼠为主要宿主动物的 HFRS 自然疫源地，在 2001—2005 年间共有肾综合征出血热病人 150 例，死亡 3 人，病死率为 2%(唐浏英等，2000；那顺孟和等，2002，2003；翟兴安等，2003；哈森高娃等，2006)。研究使用的数据及其特征、来源分别在表 1 中给出。由于 2004 年底前中国无传染病直报系统，研究使用来自大杨树镇规模最大、HFRS 病人最多的林业局医院有关 HFRS 的数据。

**表 1** 论文研究使用的数据及其特征

| 编号 | 数据名称 | 空间精度 | 时间范围 |
|---|---|---|---|
| 1 | 大杨树地区行政区划图 | 1∶250000 | 2000 年 |
| 2 | 大杨树地区林业局医院出血热病人记录数据 | | 2001—2005 年 |
| 3 | Spot vegetation | 1km | 2001—2005 年 |
| 4 | 大杨树地区 Google Earth 图像 | 30m | 2004 年 |
| 5 | 大杨树地区 Landsat 图像 | 30m | 2000 年 |

## 3 分析方法

2000—2005 年间大杨树镇 HFRS 病人数目、鼠群数目和 NDVI 值长时间序列变化之间关系研究包括两个阶段。

### 3.1 NDVI 长时间序列数据

NDVI 时序数据制备的工作流程在图 1 中给出。

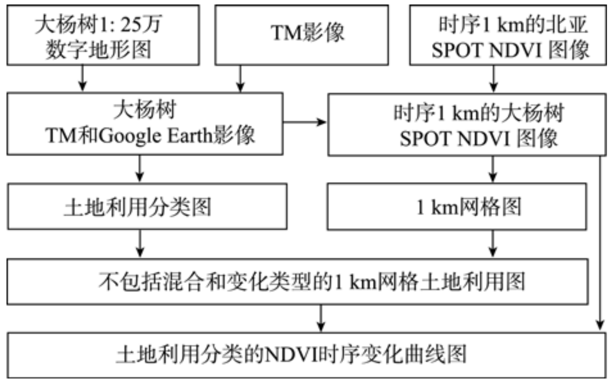


图 1 NDVI 时序数据制备的工作流程

(1) 根据经纬度坐标信息，从全国 1:25 万数字地图上截取出大杨树镇的专题图。该图包括等高线、制高点、大车道、乡村道路、县级公路、省道、国道、铁路、河流(单线河、双线河，湖泊、水库等)、村镇以及县界等信息，以 Mapinfo 格式存储。

(2) 根据大杨树的经纬度坐标，从中国科学院数据共享中心获取了大杨树地区 2000-05-27 的两景 TM 影像。经拼接处理得到了大杨树镇的 TM 影像。同时使用 Google Earth Pro 软件截取大杨树地区 2005 年的 Google Earth 图像。这两种不同时相的遥感影像用于 2001—2005 年期间的大杨树地区土地利用分类。

(3) 利用大杨树地区 2000 年的 Landsat TM 影像进行土地利用分类。分类采用监督分类和人工目视判读相结合的办法，将大杨树地区分为山地、林地、农田、居民和水体等，从而获得大杨树地区 2000 年土地利用图。基于 Google Earth 图像经过目视判读获得 2005 年大杨树地区土地利用图。

(4) 根据大杨树地区的经纬度信息，使用 SPOT-4 卫星的 Vegetation 数据。该数据主要由瑞典的 Kiruna 地面站负责接收，由位于法国 Toulouse 的图像质量监控中心负责图像质量并提供相关参数(如定标系数)，最终由位于比利时的 VITO 研究所的图像处理与存档中心负责提供下载。我们使用的是其中的 VGT-S(synthesis) S10 产品。该产品是指每 10d 合成的 4 个波段的光谱反射率及 10d 最大化 NDVI 数据集(S10)以减少云及 BRDF 的影响，SPOT 数据的预处理包括大气校正、辐射校正、几何校正、生成了 10d 最大化合成的 NDVI 数据。在文中所使用的月平均 NDVI 数值是将真实 NDVI 值乘以 100 后所得到的数值。所选 4 类地物的 NDVI 值，分布在 0—100 之间。

(5) 对大杨树地区的土地利用图与 NDVI 图进行关联分析(图 2)。鉴于栅格结构的土地利用类型图的栅格尺寸为 30m，NDVI 像元的尺寸为 1km，两者在空间上的严格配准是工作的基础和需要解决的首要问题。为此，利用经纬度坐标使大杨树镇地区的土地利用类型图与 NDVI 图准确地重叠；根据 NDVI 图的像元矩阵生成相应的 1km 格网，使之叠置在土地利用类型图上，从中选择网格中为单一或近似单一(其他类型面积不大于 5%)的土地类型图斑，作为网格 NDVI 值与其相应土地利用类型的关联样本；从为数众多的山地、林地、农田和居民点的关联样本中，随机地各选取 10 个样本，分别建立土地利用类型与 NDVI 值之间有代表性的对应关系；每种土地利用类型有代表性的 NDVI 值随时间的演进不断

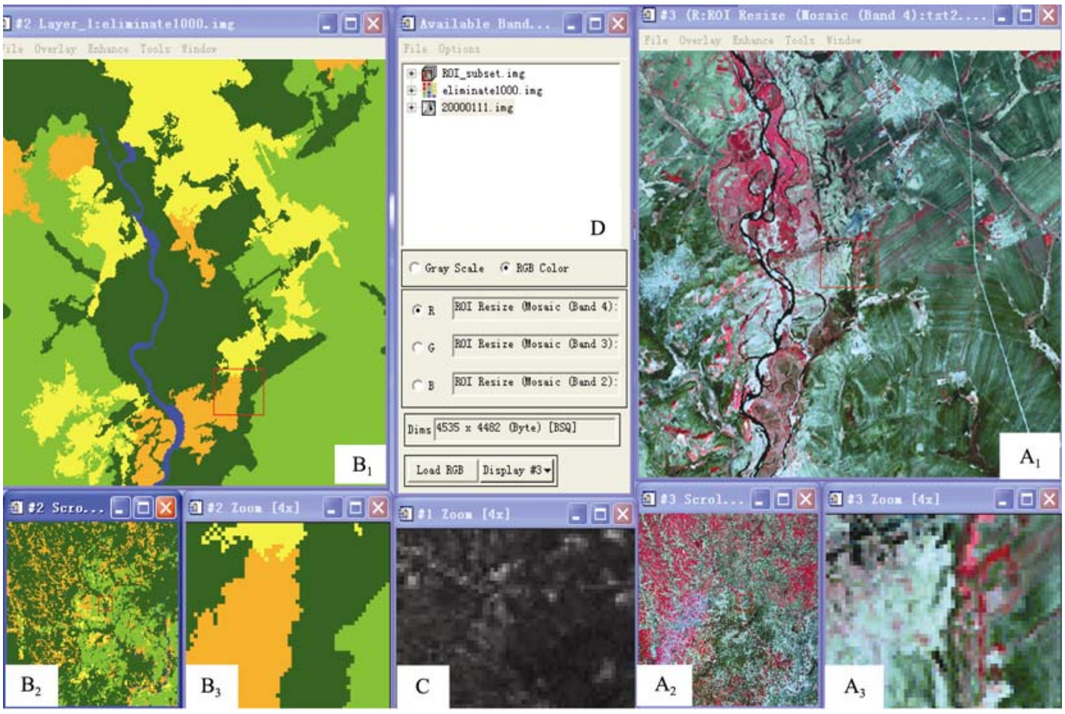


图 2 大杨树镇 NDVI 图像与 TM 影像及其土地利用判读地图的关联互动
$A_1$、$A_2$、$A_3$ 分别是大杨树镇的 TM 放大、全景及窗口影像; $B_1$、$B_2$、$B_3$ 分别是相应的 TM 影像土地利用判读放大、全景及窗口专题图; C 是大杨树镇的 NDVI 图像; D 是构建影像及其判读地图之间相互关联、互动的对话框；像、图上的红线方框，是根据需要而专门挑选出来的窗口区域

变化, 据此可以分别绘制出它们的 NDVI 时序变化曲线。在本研究中, 选择月份为时间单位, 每月的 NDVI 值用 3 个旬的 NDVI 平均值表示。鉴于大杨树镇地区的土地利用状况多年来一直比较稳定, 2000 年 TM 影像的土地利用类型判读图, 可用以代表其 2001—2003 年土地利用状况, 2005 年 Google Earth 图像的土地利用类型判读图, 可用以代表其 2004 年、2005 年的土地利用状况。这样, 就可获得大杨树镇地区山地、林地、农田和居民点及其相应的月平均 NDVI 值在 2001—2005 年期间的时序变化曲线图。

### 3.2　HFRS 与 NDVI 时间关系分析方法

HFRS 病人数目与 NDVI 值时序变化之间的相互关系分析研究按以下 3 个步骤进行: 首先, 采用图解叠加的直观比较方法, 寻找两者之间的时间关系; 其次, 采取曲线错位的相关计算方法, 确立它们之间的时间关系; 最后, 建立 HFRS 病人数目与最佳错位 NDVI 值的定量关系模型。

(1) 利用时相总数为 60 个月的月平均 NDVI 数据, 分别绘制出大杨树地区山地、林地、农田、居民点等地类在 2000—2005 年间的 NDVI 变化曲线。与此同时, 按月份绘制出表示大杨树镇林业局医院 HFRS 病人数目同期变化的柱状图。然后, 使它们在同一时间坐标轴上叠合, 可以获得图 4 上部的 NDVI-HFRS 病人数变化比较图。同理, 在 2000—2005 年 HFRS 病人数变化柱状图上, 可以分别点绘黑线姬鼠和褐家鼠密度曲线, 获得图 3 下部的鼠密度- HFRS 病人数变化比较图。

(2) 以大杨树镇 HFRS 月发病人数的时序变化作为参考图, 分别绘制与它同期(后错 0 个月)和向后错位 1、2、3、4、5 和 6 个月的月平均 NDVI 值的时序曲线图, 由此可得与 HFRS 月发病人数配对的 7 个月平均 NDVI 值的时序数组(图 4)。在此基础上, 分别对山地、林地、农田和居民点等 4 种土地利用类型的 7 个配对的月平均 NDVI 值时序数组与 HFRS 月发病人数的时序数组进行相关分析。其分析结果的相关系数和 $P$ 值在表 2 中分别给出。可以看出农田、山地和居民点后错 3 个月的时序数组与 HFRS 月发病人数的时序数组的相关系数分别为 0.67、0.63 和 0.61; 山地和林地后错 4 个月的数组与月发病人数的数组之间的相关系数均为 0.66。

(3) 鉴于农田比较靠近居民点、地势平坦、自然条件单一, 而且其后错 3 个月的月平均 NDVI 值与 HFRS 月发病人数的相关系数最高, 故选择它们建立月平均 NDVI 值与 HFRS 月发病人数之间的定量关系模型。利用线性回归方法得到的模型为 $y=0.212+0.073x$。其中, $y$ 代表 HFRS 月发病人数, $x$ 代表后错 3 个月的 NDVI 月平均值。这种结果可以用 HFRS 月发病人数与后错 3 个月的月平均 NDVI 值的散点图以及其两者拟合出来的直线表达(图 5)。

## 4　结果讨论

大杨树镇是以农业和林业为主要产业的地区。根据对当地卫生部门以及土地规划部门的调查得知: 自 2000 年以来大杨树地区实行了封山育林政策, 林区面积基本没有变化, 农田面积及其主要农作物种类(大豆)也没有明显的变化。因此, 可以利用 2000 年和 2005 年的土地利用判读图, 分别代表 2001—2003 年和 2004—2005 年的土地利用状况。

从时序 HFRS 发病人数与相应鼠密度、NDVI 值的图解叠加方法得到的形象、直观的结果(图 3)看出: 山地、林地、农田和居民点的 NDVI 变化的高峰值出现在每年的 8 月份, 黑线姬鼠密度的峰值大多出现在每年的 9 月份, 褐家鼠密度较小而且在一年四季里没有明显的峰值出现, 而 HFRS 病人数的高峰值出现在每年的 11 月份。由此可见, HFRS

表 2　**HFRS** 月发病人数与配对 **NDVI** 月平均值的相关分析结果

| 地类 | 参数 | 后错 0 个月 | 后错 1 个月 | 后错 2 个月 | 后错 3 个月 | 后错 4 个月 | 后错 5 个月 | 后错 6 个月 |
|---|---|---|---|---|---|---|---|---|
| 山地 | 相关系数 | −0.31 | −0.07 | 0.34 | 0.63 | 0.66 | 0.46 | 0.11 |
| | $P$ 值 | 0.01 | 0.60 | 0.01 | 0 | 0 | 0 | 0.41 |
| 林地 | 相关系数 | −0.34 | −0.06 | 0.33 | 0.57 | 0.66 | 0.47 | 0.10 |
| | $P$ 值 | 0.01 | 0.64 | 0.01 | 0 | 0 | 0 | 0.44 |
| 农田 | 相关系数 | −0.31 | −0.02 | 0.43 | 0.67 | 0.59 | 0.37 | 0.06 |
| | $P$ 值 | 0.02 | 0.90 | 0 | 0 | 0 | 0 | 0.64 |
| 居民点 | 相关系数 | −0.32 | −0.02 | 0.38 | 0.61 | 0.55 | 0.32 | 0.04 |
| | $P$ 值 | 0.01 | 0.86 | 0 | 0 | 0 | 0.01 | 0.74 |

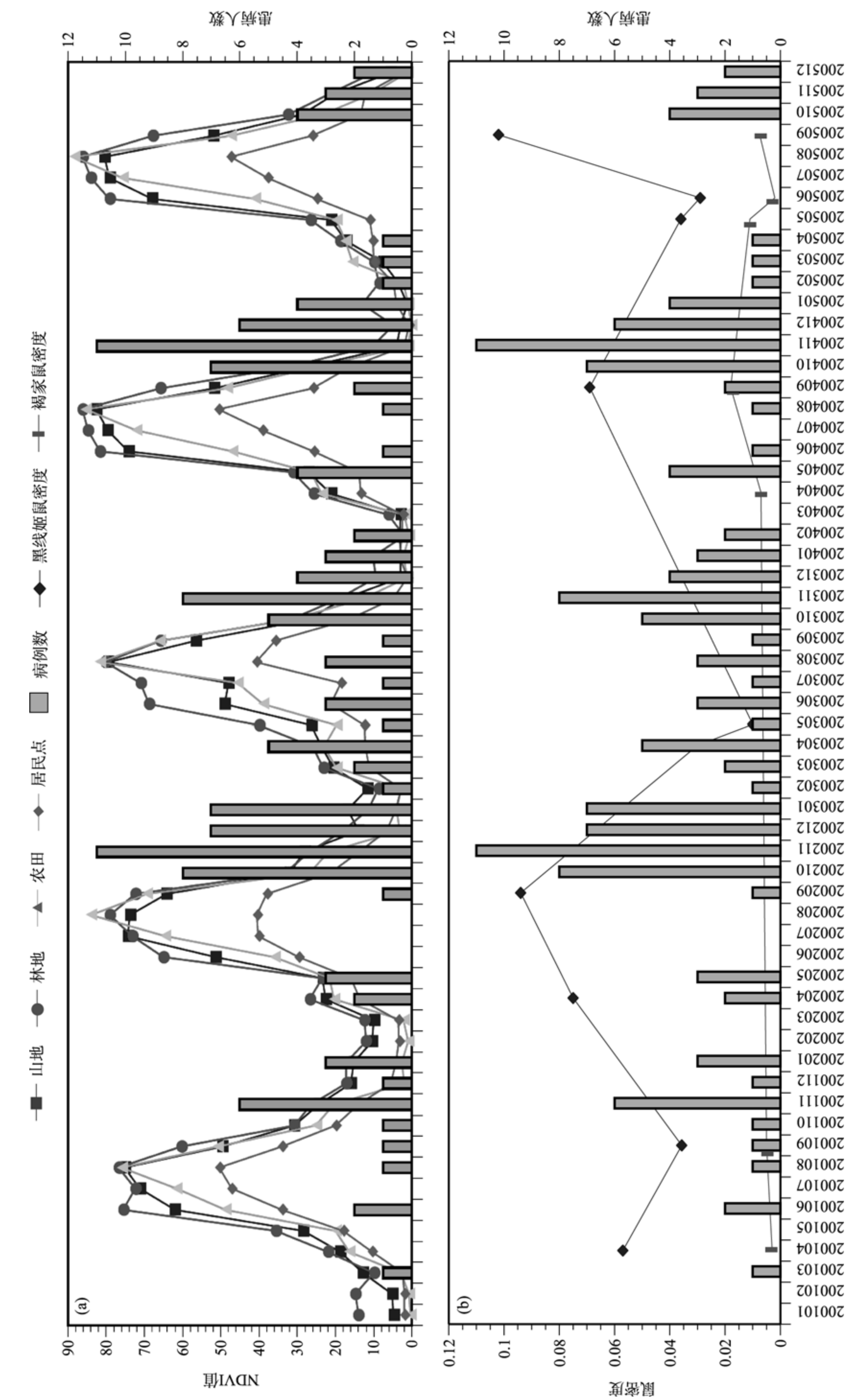


图 3 大杨树镇 NDVI、鼠密度、HFRS 病人数变化关系的比较图(2001—2005)

(a) NDVI-HFRS 病人数变化比较图; (b) 鼠密度—HFRS 病人数变化比较图

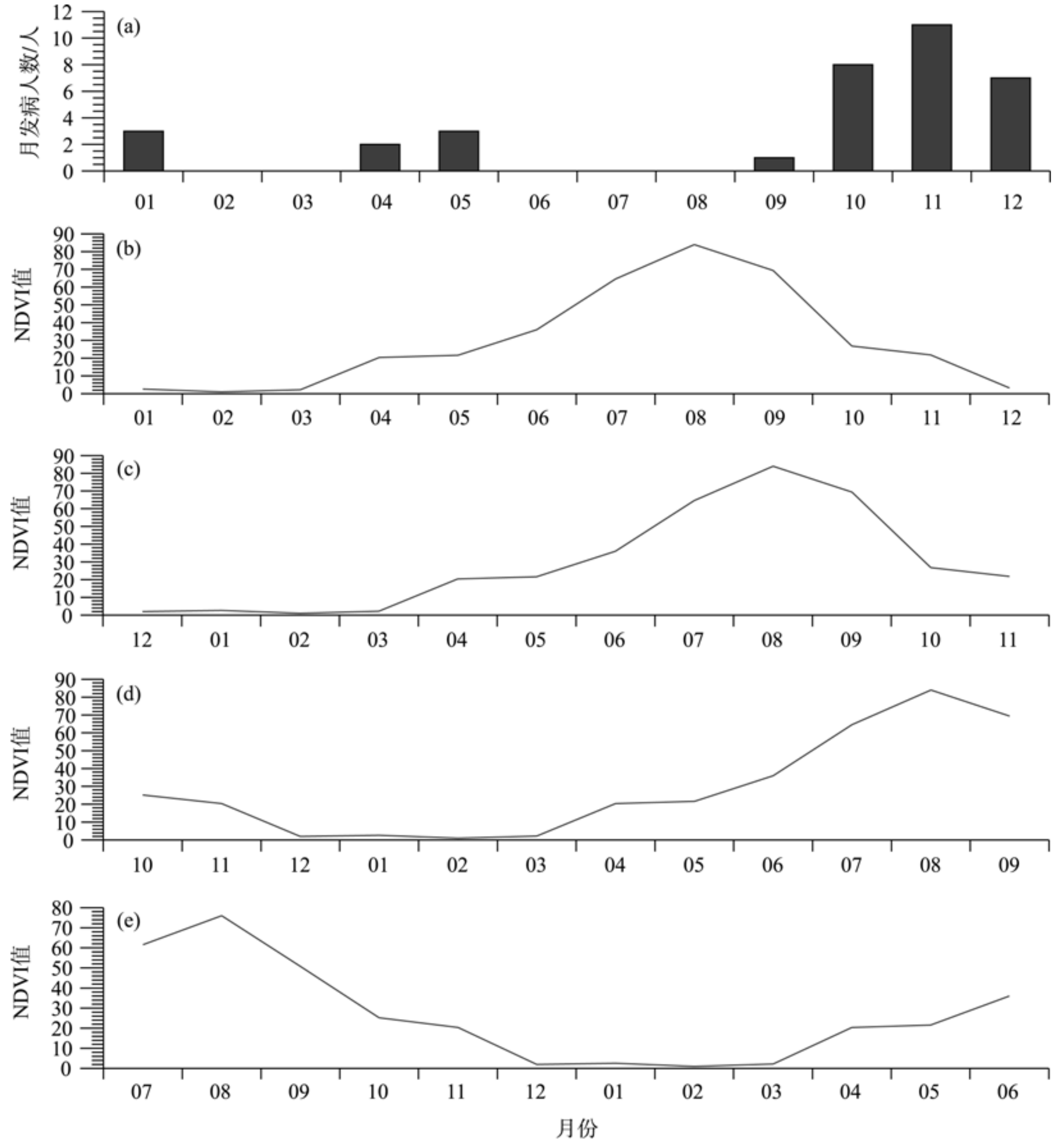


图 4　HFRS 月发病人数与错位月平均 NDVI 值的时序图组
(a) HFRS 病人数; (b)后错 0 个月; (c)后错 1 个月; (d)后错 3 个月; (e)后错 6 个月

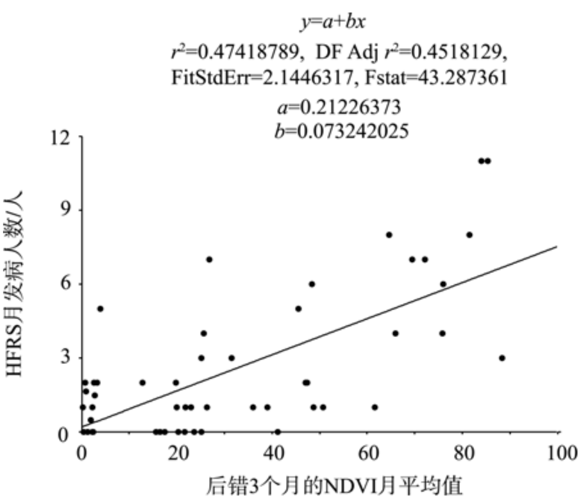


图 5　HFRS 月发病人数与后错 3 个月的 NDVI 月平均值的关系模型

发病人数变化过程滞后于黑线姬鼠密度变化过程大约 2 个月时间, 滞后于 NDVI 变化过程大约 3 个月时间。从时序 HFRS 发病人数的数组和与之配对的错位时序月平均 NDVI 值数组的相关分析计算结果(表 2)表明: HFRS 发病人数变化过程滞后于农田和居民点的 NDVI 变化过程 3 个月时间, 滞后于山地的 NDVI 变化过程 3—4 个月时间, 滞后于林地的 NDVI 变化过程 4 个月时间。尽管这两种方法得到的结果存在差异, 但就其总体态势及其今后使用的需要而言, 得出 HFRS 发病人数的变化过程滞后于月平均 NDVI 值的变化过程至少 3 个月时间是比较合理的, 可以作为 HFRS 的遥感早期报警的一个重要参考依据。

利用 HFRS 月发病人数与后错 3 个月的农田

NDVI 月平均值的配对时序数据组，建立了大杨树镇地区 HFRS 月发病人数的线性回归模型。它描述了在以黑线姬鼠为主要宿主动物的大杨树镇自然疫源地里, HFRS 与农田 NDVI 之间的数量关系。这个模型可以用大杨树镇农田的某个月平均 NDVI 值推算其后第 3 个月的 HFRS 月发病人数。论证了研制和应用 HFRS 遥感早期报警系统的可行性。研究成果在大杨树镇试验区的实用化尚需要使用更长时序的配对数据进行调整和改进；在试验研究区以外推广应用，更需要在全国不同类型的 HFRS 疫区里开展深入的试验研究，以修改、扩充甚至重建这个模型。本研究将会促进 HFRS 遥感早期报警系统的研制，最终使之在中国 HFRS 的预防和控制工作中得到具体而有效的应用。

## REFERENCES


Boone J D, McGwire K C, Otteson E W, DeBaca R S, Kuhn E A, Villard P, Brussard P F and St Jeor S C. 2000. Remote sensing and geographic information systems: charting Sin Nombre virus infections in deer mice. *Emerging Infectious Diseases.*, **6**(3): 248—258

Fang L Q, Cao W C, Chen H X, Wang B G, Wu X M Yang H and Zhang X T. 2003.Study on the application of geographic information system in spatial distribution of hemorrhagic fever with renal syndrome in China. *Chinese Journal of Epidemiology*, **24**(4): 265—270

Fang L Q, Cao W C, Dong Z, Wu X M, Sun P Y, Martin Kulldorff, Wang B C, Yang H and Li X W. 2003. Spatial analysis on the distribution of hemorrhagic fever with renal syndrome by geographic information system in Haidian district, Beijing. *Zhonghua Liu Xing Bing Xue Za Zhi*, **24**(11): 1020—1023

Fang L Q, Li C Y, Yang H, Wu X M, Yang H, Chen H X, Li X W and Cao W C. 2003. Using geographic information system to study on the association between epidemic areas and main animal hosts of hemorrhagic fever with renal syndrome in China. *Chinese Journal of Epidemiology*, **25** (11): 929—933

Glass G E, Cheek J E, Patz J A, Shields T M, Doyle T J, Thoroughman D A, Hunt D K, Enscore R E, Gage K L, Irland C, Peters C J and Bryan R. 2000. Using remotely sensed data to identify areas at risk for hantavirus pulmonary syndrome. *Emerging Infectious Diseases*, **6**(3): 238—247

Nashun Menghe and Chen Y G. 2002. On Forest Classification Management in Dayangshu District *Inner Mongolia Forestry Investation and Design*, **25**(1): 47—48

Nashun Menghe and Li X L. 2000. Protection policy of forest resources in Dayangshu bureau of forest. *Inner Mongolia Forestry Investation and Design*, **24**(3): 21—23

Sasen Gaowa Li C P, Wu S B and Wang J B. 2006. Population structural changesin hemorrhagic fever with renal syndrome patients at Inner Mongolia Xing’an forest area. *Chinese Journal of Pest Control*, **22**(4): 264—265

Song G. 1998. Manual of Hemorrhagic Fever with Renal Syndrome Control and Prevention. Beijing People’s Medical Publishing House

Tang L Y, Chen H X, Zou X Y, Luo C W, Yu T, Dong J J, Kang F C and Zhao L Y. 2000. A Surveillancestudy on the enzoonostic natural of HFRS (Hemorrhagic Fever with Renal Syndrome) in Dayangshu district of Elunchun autonomic county. *Chinese Journal of Zoonoses*, **16**(6): 89—90

Yan L. 2007. Ecological Study on Hemorrhagic Fever with Renal Syndrome in China based on Spatial Information technology. Chinese Science of Academy

Yan, L, Fang L Q , Huang H G, Zhang L Q, Feng D, Zhao W J, Zhang W Y, Li X W and Cao W C. 2007. Relationship between landscape elements and Hantaan virus-related hemorrhagic fever with rental syndrome in China. *Emerging Infectious Diseases*, **13**(9): 1301—1306

Zhai X A and Wang L K. 2003. Suggestion on returning cropland back to forestry in Dayangshu Forestry Bureau, Inner Mongolia. *Inner Mongolia Forestry Investation and Design*, **26**(2): 49—50

Zhi H. 1998, Epidemiology. Beijing People’s Medical Publishing House


### 附中文参考文献


方立群，曹务春，陈化新，王宝光，吴晓明，杨红，张习坦. 2003. 应用地理信息系统分析中国肾综合征出血热的空间分布. 中华流行病学杂志, **24**(4): 265—270

方立群，曹务春，敦哲，吴晓明，孙培源，Martin Kulldorff，王炳才，杨红，李小文. 2003. 应用地理信息系统分析北京市海淀区肾综合征出血热的空间分布. 中华流行病学杂志，**24**(11): 1020—1023

方立群，李承毅，杨华，吴晓明，杨红，陈化新，李小文，曹务春. 2004. 应用地理信息系统研究我国肾综合征出血热疫区类型与主要宿主动物构成的关系. 中华流行病学杂志，**25**(11): 929—933

哈森高娃，李春甫，吴松波，王剑波. 2006. 内蒙古大兴安林区肾综合征出血热人群结构变化特征. 医学动物防制，**22**(4): 264—265

那顺孟和，陈永革. 2002. 对大杨树地区森林分类经营的探讨. 内蒙古林业调查设计, **25**(1): 47—48

那顺孟和，李雪林. 2001. 大杨树林业局森林资源的保护对策. 内蒙古林业调查设计, **24**(3): 21—23

宋干, 1998. 流行性出血热防治手册. 第2版. 北京：人民卫生出版社

唐浏英，陈化新，邹学义，罗成旺，余陶，董俊杰，康凤春，赵林英. 2000. 鄂伦春自治旗大杨树镇肾综合征出血热自然疫源地性质调查研究. 中国人兽共患病杂志, **16**(6): 89—90

闫磊. 2007. 基于空间信息技术的肾综合征出血热景观流行病学研究. 北京：中国科学院

翟兴安，王连宽. 2003. 对内蒙古大杨树林业局退耕还林工作的建议. 内蒙古林业调查设计, **26**(2): 49—50

志浩. 1994. 流行病学. 第三版. 北京：人民卫生出版社